Two-Step Finite-Control Set Model Predictive Control for Three Phase UPS Inverters Feeding Non-linear Loads

Youssuf Elthokaby
Faculty of Engineering at Shoubra, Benha University, Egypt
youssef.hassan@feng.bu.edu.eg

Naser Abdel-Rahim
Future University in Egypt
naser.abdelrahim@fue.edu.eg

Keywords: <<Converter circuits>>, <<Uninterruptible Power Supply (UPS)>>, <<Control methods for electrical systems>>

Abstract: A two-step prediction horizon finite-control set model predictive control scheme is proposed for three phase UPS inverters. Within the control scheme, a constraint is implemented to limit the maximum inverter inrush current, in case of non-linear loads, to an acceptable value. Simulation results show that the proposed control scheme has been successful in limiting the inrush current and producing a load voltage with very low THD with small filter size.

I. INTRODUCTION

Critical loads such as medical facilities, computer systems, and emergency equipment need continuous power supply to avoid severe impact on them. Uninterruptable power supply (UPS) is usually used to supply these loads where a Voltage Source Inverter (VSI) provides reliable and high-quality output sinusoidal voltage. An LC filter is connected to remove high order harmonic components. However, this filter increases the complexity of the system controller design. Many control strategies have been applied to generate the output voltage of the VSI, including PI, resonant, repetitive, deadbeat and predictive controllers [1]-[7].

Predictive control provides a wide class of controllers. They can be classified as hysteresis-based, trajectory-based, deadbeat-based and model-based predictive controllers [8]. The controlled variable with hysteresis-based predictive control attempts to be in the boundary of the hysteresis area. The hysteresis area location is identified by the reference signal of the controlled variable. When the controlled variable reaches the boundary, the controller predicts the controlled variable for each possible switching state. Then, optimization is used to select the next switching state [9].

Trajectory-based predictive control is widely used in electric motor drives. The controller chooses the switching state that forces the system variables to be onto pre-calculated trajectories. It includes techniques such as direct self-control[10], direct mean torque control [11], and direct speed control[12]. Hysteresis-based and trajectory-based predictive control do not need a modulator to generate the switching state. Hence, the output of the controller itself is the gating signals of the power semiconductor switches.

Deadbeat-base predictive control uses the model of the system to get the control signal that makes the controlled variable reach its reference value. The control signal is then applied to a modulator to generate the switching signals. The disadvantage of this method is that it becomes more complex if it includes nonlinearities or constraints [8].

The inite-control set model predictive control (FCS-MPC) proposed in this paper is more suitable for the discrete nature of the power electronics converters and lends itself easily to its application. In FCS-MPC, the optimization problem is reduced to the number of possible switching states of the power converter. The cost function is used to select the switching state that minimizes it [13]-[18]. The comparison between FCS-MPC using 1-step and 2-step prediction horizon has been presented in [19]. However, with FCS-MPC, the number of steps would not exceed two since, while the performance will not further improve, the computational burden would drastically increase[19], [20]. This is because one voltage vector is applied during the first sampling instant and another voltage vector is applied during the second sampling instant. This problem is solved in [19] by applying the same voltage vector for several sampling instants. The performance and THD of the output voltage for both the one- and two-step prediction horizon are very similar.

This paper proposes the application of a two-step prediction horizon FCS-MPC scheme to three-phase UPS inverters. The scheme implements a constraint within the controller to limit the maximum

inverter current to its steady-state value. This gives the controller the advantage of protecting the power switching devices against high surges of inverter output current, especially in case of non-linear loads, while maintaining well-regulated output voltage with very low THD. While the FCS-MPC with two-step prediction horizon used to control three-phase UPS inverter has been reported in the literature, the performance of the three-phase UPS system with two-step FCS-MPC and constraint has not been reported.

II. SYSTEM MODELLING

The power circuit of a three-phase inverter with second-order LC filter at its output is shown in Fig. 1. The modeling of the three-phase inverter and the output LC filter are presented in this section. The switching states of the three-phase inverter are defined by gating signals L_a, L_b, and L_c as follows:

$$L_a = \begin{cases} 0 \ if \ Q_1 OFF \ and \ Q_4 ON \\ 1 \ if \ Q_1 ON \ and \ Q_4 OFF \end{cases} \quad (1)$$

$$L_b = \begin{cases} 0 \ if \ Q_3 OFF \ and \ Q_6 ON \\ 1 \ if \ Q_3 ON \ and \ Q_6 OFF \end{cases} \quad (2)$$

$$L_c = \begin{cases} 0 \ if \ Q_5 OFF \ and \ Q_2 ON \\ 1 \ if \ Q_5 ON \ and \ Q_2 OFF \end{cases} \quad (3)$$

Equations (1)-(3) can be expressed in vector form:

$$\boldsymbol{L} = \frac{2}{3}\left(L_a + \boldsymbol{a} L_b + \boldsymbol{a}^2 L_c\right) \quad (4)$$

Where $\mathbf{a} = e^{j\frac{2\pi}{3}} = -\frac{1}{2} + j\frac{\sqrt{3}}{2}$ represents the 120° phase displacement between the phases. The phase voltages with respect to the negative terminal of dc-link N are defined by these gating signals as follows:

$$\begin{aligned} v_{aN} &= L_a V_{dc} \\ v_{bN} &= L_b V_{dc} \\ v_{cN} &= L_c V_{dc} \end{aligned} \quad (5)$$

The output voltage vector is defined by:

$$\boldsymbol{v}_i = \frac{2}{3}\left(v_{aN} + \boldsymbol{a} v_{bN} + \boldsymbol{a}^2 v_{cN}\right), \quad (6)$$

So $\boldsymbol{v}_i = V_{dc}\boldsymbol{L}$.

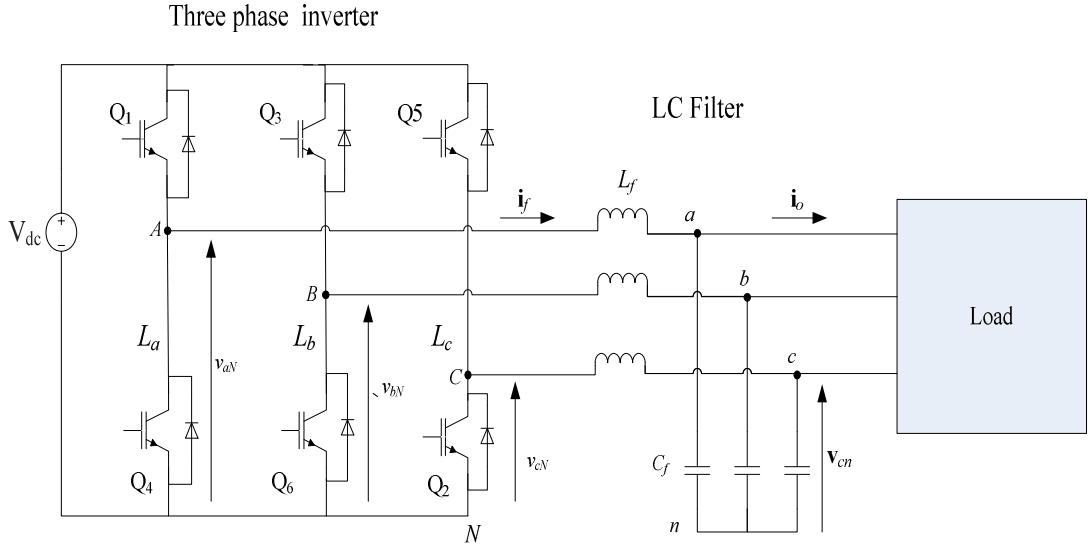

Fig. 1. Three phase-inverter with output LC filter system

In this way, the different combinations of the gating signals L_a, L_b, and L_c can only generate eight possible switching states. Consequently, eight voltage vectors can be obtained from the three-phase inverter as shown in Fig. 2. The three-phase inverter can be considered as a linear discrete system with only 7 different voltage vectors as there are two voltage vectors equal to zero $\mathbf{v}_0$=$\mathbf{v}_7$=0.

A. Modelling with the LC filter

The output LC filter is used to eliminate high order harmonic content in the output voltage and current. The load voltage, $\boldsymbol{v}_c$, the inductor filter current, $\boldsymbol{i}_f$, and the load current, $\boldsymbol{i}_o$, are given by:

$$\boldsymbol{v}_c = \frac{2}{3}\left(v_{ca} + \boldsymbol{a} v_{cb} + \boldsymbol{a}^2 v_{cc}\right) \quad (7),$$

$$\boldsymbol{i}_f = \frac{2}{3}\left(i_{fa} + \boldsymbol{a} i_{fb} + \boldsymbol{a}^2 i_{fc}\right) \quad (8),$$

$$\boldsymbol{i}_o = \frac{2}{3}\left(i_{oa} + \boldsymbol{a} i_{ob} + \boldsymbol{a}^2 i_{oc}\right) \quad (9).$$

The governing differential equations of the LC filter are:

$$L_f \frac{d\boldsymbol{i}_f}{dt} = \boldsymbol{v}_i - \boldsymbol{v}_c \quad (10),$$

$$C_f \frac{d\boldsymbol{v}_c}{dt} = \boldsymbol{i}_f - \boldsymbol{i}_o \quad (11),$$

where L_f and C_f are the filter inductance and capacitance, respectively. Equations (10) and (11) can be rewritten in a state-space variable format as:

$$\frac{d\boldsymbol{x}}{dt} = A\boldsymbol{x} + B\boldsymbol{v}_i + B_d \boldsymbol{i}_O, \quad (12),$$

where

$$\boldsymbol{x} = \begin{bmatrix} \boldsymbol{i}_f & \boldsymbol{v}_C \end{bmatrix}^T \quad (13),$$

$$A = \begin{bmatrix} 0 & \frac{-1}{L_f} \\ \frac{1}{C_f} & 0 \end{bmatrix} \quad (14),$$

$$B = \begin{bmatrix} \frac{1}{L_f} \\ 0 \end{bmatrix} \quad (15),$$

$$B_d = \begin{bmatrix} 0 \\ \frac{-1}{C_f} \end{bmatrix} \quad (16).$$

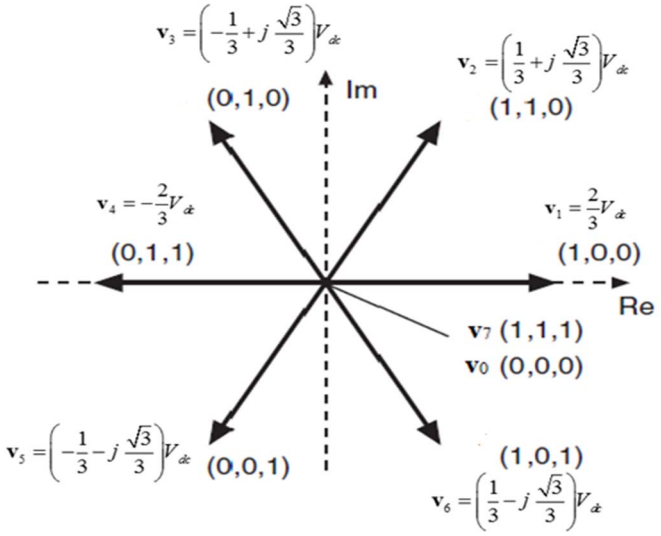

Fig. 2. Voltages vectors of the three-phase inverter

The system output equation is given by:

$$\boldsymbol{v}_c = [0 \quad 1]\boldsymbol{x} \tag{17}$$

B. The discrete time model of the system

The discrete time model is used to predict the future behaviour of the controlled variables. It is obtained from (12) for a sampling time T_S and expressed as:

$$\boldsymbol{x}(k+1) = A_q \boldsymbol{x}(k) + B_q \boldsymbol{v}_i(k) + B_{dq} \boldsymbol{i}_o(k) \tag{18},$$

where

$$A_q = e^{AT_S} \tag{19},$$

$$B_q = \int_0^{T_s} e^{At} B dt \tag{20},$$

$$B_{dq} = \int_0^{T_s} e^{At} B_d dt \tag{21}.$$

Referring to (13) and (18), it can be seen that the output voltage, $\boldsymbol{v}_c$, is predicted from the voltage vectors, $\boldsymbol{v}_i$, which depends on the switching states, the measured inverter output voltages, and the inductor filter currents at the k[th] sampling instant.

III. PROPOSED PREDICTIVE CONTROL STRATEGY

The proposed control algorithm is the finite-control set model predictive control (FCS-MPC). The FCS-MPC has all the advantages of continuous-control set model predictive control. For instance, it is easy to understand, can deal with multivariable systems and nonlinearities, and can set constraints on the system variables within a cost function. In addition, it lends itself easily to the implementation of power electronics converters.

The value of the output voltage at next instance $\boldsymbol{v}_c$(k+1) can be predicted using (18). The value of the output voltage, $\boldsymbol{v}_c$(k), inductor filter current, $\boldsymbol{i}_f$(k), and the output current, $\boldsymbol{i}_o$(k), are measured at the current instance k. Seven values of $\mathbf{v}_c$(k+1) are obtained for each possible switching state of the inverter. Then, it can be estimated which of the voltage vectors of the inverter $\boldsymbol{v}_i$ gives value of $\boldsymbol{v}_c$(k+1), which is the nearest to the reference value. Consequently, the corresponding switching state is applied in the next instance.

The cost function is used to select the optimal switching state that gives the lowest error between reference and output voltages at next instance. The cost function is defined as:

$$g_1 = \left(v^*_{c\alpha} - v_{c\alpha}(k+1)\right)^2 + \left(v^*_{c\beta} - v_{c\beta}(k+1)\right)^2, \tag{22}$$

where $v_{c\alpha}$ and $v_{c\beta}$ are the real and imaginary parts of the predicted output voltage vector $\boldsymbol{v}_c$(k+1). Constraints can be easily added to the cost function as will be shown later.

The Two-step prediction horizon

In the previous discussion, only one-step prediction horizon is considered. In this section two-step prediction horizon is proposed. In two-step prediction horizons, the value of output voltage $\boldsymbol{v}_c$(k+2) is given by

$$\boldsymbol{x}(k+2) = A_q \boldsymbol{x}(k+1) + B_q \boldsymbol{v}_i(k) + B_{dq} \boldsymbol{i}_o(k) \tag{23}.$$

In (23), the inverter output current, $\boldsymbol{i}_o$(k), is considered to be changing slowly with respect to the sampling time, so its value at the instant (k+1) is the same as that at sample k.

With two-step prediction horizon, one voltage vector is applied during the prediction of the first step, $\boldsymbol{x}(k+1)$, and another voltage vector is applied during the prediction of the second step, $\boldsymbol{x}(k+2)$. This leads to 8^2=64 possible sequences of the two voltage vectors calculations, which results in a heavy computational burden. To reduce the number of calculations, the inverter voltage vector used in the prediction of the first step is also employed to predict the state variables of the second step. This is instead of using two different inverter voltage vectors. It was shown in [20] that with only two-step

prediction horizon, this approximation produces almost the same results as that when using two different voltage vectors.

The cost function is modified to be as in (24). The reference value is assumed constant at all instants.

$$g_2 = \left(v^*_{c\alpha} - v_{c\alpha}(k+2)\right)^2 + \left(v^*_{c\beta} - v_{c\beta}(k+2)\right)^2 \quad (24).$$

IV. SIMULATION RESULTS WITH TWO-STEP PREDICTION HORIZON

The proposed controller is simulated using MATLAB/Simulink and the load parameters are given in Table I.

Table I: Simulation Parameters

DC source (V_{dc})	500 V
The peak value of the reference phase voltage	$500/\sqrt{3}$ V (max)
Frequency of the reference voltage	50 Hz
Sampling time (T_S)	50 µsec
Filter capacitor C_f	100 µf
Filter inductor L_f	2 mH
Output resistance R	50 Ω
DC side capacitance C_{dc}	2200 µf
DC side inductance L_{dc}	10 mH

A. Results of two-step prediction horizon and non-linear load

The controller behaviour is simulated with non-linear load. The non-linear load is chosen as a three-phase diode bridge rectifier with LC filter in DC side as shown in Fig. 3.

The output voltages ($\boldsymbol{v}_c$) waveforms of the three phases are shown in Fig. 4. The output voltages are sinusoidal with low THD equals 2.43%. The peak value of the output voltage for any phase at steady-state is 283 V. The figure shows that the output voltages take a half cycle to reach steady state operation. The inductor filter currents of the three phases ($\boldsymbol{i}_f$) are shown in Fig. 5. These currents have a high value at starting point. A constrain can be set, within the control algorithm, to limit the value of the maximum inverter output currents. The output DC voltage from the bridge rectifier (V_{odc}) is shown in Fig. 6. The output DC voltage has an average value equal to 461.5 V with ripples (peak to peak) of 11.7 V (i.e. 2.54%). The DC output voltage has a starting overshoot value reaching as high as 598 V.

B. Results with two-step prediction horizon with non-linear load and constraint

The MPC algorithm lends itself easily to implementing such a constraint which is added to the cost function as:

$$g_2 = \left(v^*_{c\alpha} - v_{c\alpha}(k+2)\right)^2 + \left(v^*_{c\beta} - v_{c\beta}(k+2)\right)^2 + h \quad (25),$$

where "h" is a penalty factor. In this work, "h" is set to infinity when the inductor currents, $\boldsymbol{i}_f$, exceeds its maximum steady-state value ($i_{f,max}$=30 A). And if $\boldsymbol{i}_f$ is less than or equal to $i_{f,max}$, "h" is set to zero. Now, the controller chooses the voltage vector that minimizes the error between the output voltage and its reference while the inductor currents are lower than $i_{f,max}$.

The three-phase inductor filter currents are shown in Fig. 7. Here, the inductor filter currents are limited to i_{max} at starting. Fig. 8 shows the output voltages of the three phases. The output voltages are nearly sinusoidal with THD equal to 2.49% at steady state. The peak value of the output voltages is 282.5 V with a line-line peak value of 488.4 Volts (VUR=97.7%). The figure shows that the output voltages take approximately two cycles to reach its steady state operation. At the first two cycles, the output voltages are highly distorted because the constraint is active as shown in Fig. 7. Then, the inductor filter currents are lower than i_{max} so, the constraint becomes inactive. The bridge rectifier output DC voltage (V_{odc}) is shown in Fig. 9. The DC output voltage takes 50 milliseconds to reach its steady state

value. However, it does not experience any overshoot at starting. The mean value of V_{odc} is 462.6 V with ripples (peak to peak) equals 11.2 V, i.e. 2.42%.

The switching energy losses of a switch can be calculated from a polynomial of the switched voltage and current in (26), where k_1, k_2,…, k_5 are derived from a least-square approximation of measured data [21]. For simplicity, some terms of the polynomial can be neglected and only the first term is considered[22]. So, the energy losses are expressed as in (27). The IGBT model NGTB40N60IHLWG is used for the analysis which has ratings of 600 V and 40 A [23]. The switch turn-on delay time and rise time are 0.11 µs, and the turn off delay time and fall time are 0.21 µs at 25°c. A maximum value of T_c is taken equal to 0.3 µs. The switched current is the same as that in the inductor filter and the switched voltage is the line-to-line voltage between the input phases involved in the commutation. The switching energy losses are shown in Fig. 10. The switching losses are increased when the constraint is active yet reduced when the constraint is inactive. Hence, the efficiency has a low value when the constraint is active and is as high as 95% in steady state operation. The efficiency of the system is shown in Fig. 11.

$$E_L = k_1 \Delta i_s \Delta v_s + k_2 \Delta i_s \Delta v_s{}^2 + k_3 \Delta i_s{}^2 \Delta v_s + k_4 \Delta v_s{}^2 + k_5 \Delta i_s{}^2 \Delta v_s{}^2 \quad (26)$$

$$E_L = k_1 \Delta i_s \Delta v_s = \int_{T_c} p(t)dt = \int_{T_c} i_s(t) v_s(t)dt = \frac{T_c}{6} \Delta i_s \Delta v_s \quad (27)$$

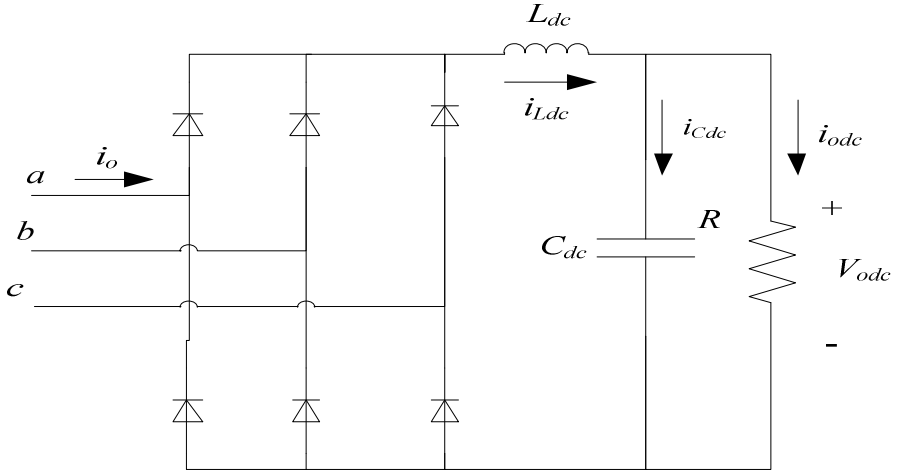

Fig. 3. Non-linear load

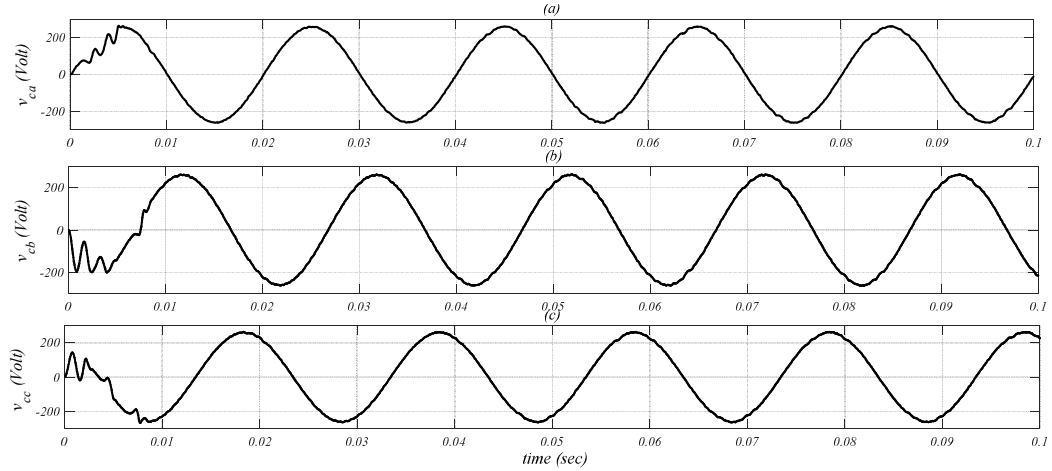

Fig. 4. The output voltage ($\boldsymbol{v}_c$) of the three phases with non-linear load (a) phase a, (b) phase b, (c) phase c

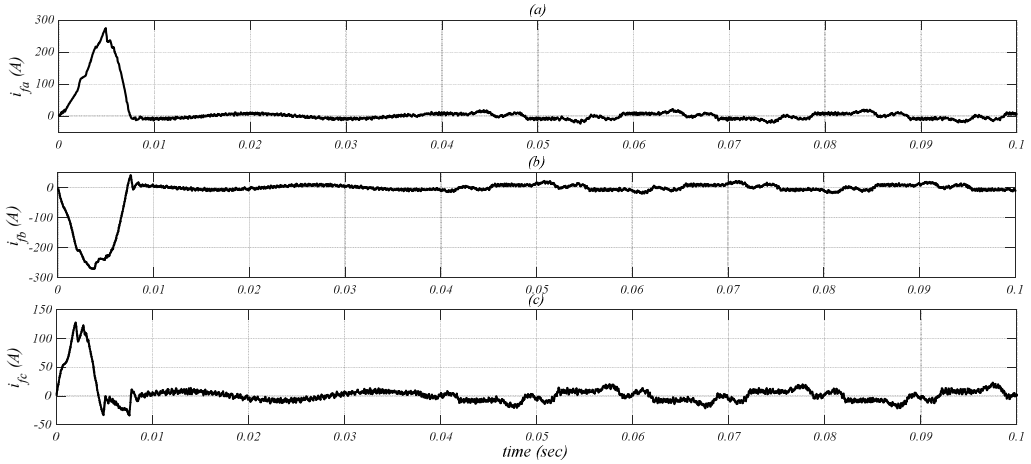

Fig. 5. The inductor filter current ($\boldsymbol{i_f}$) of the three phases with non-linear load Phase a, (b) phase b, (c) phase c

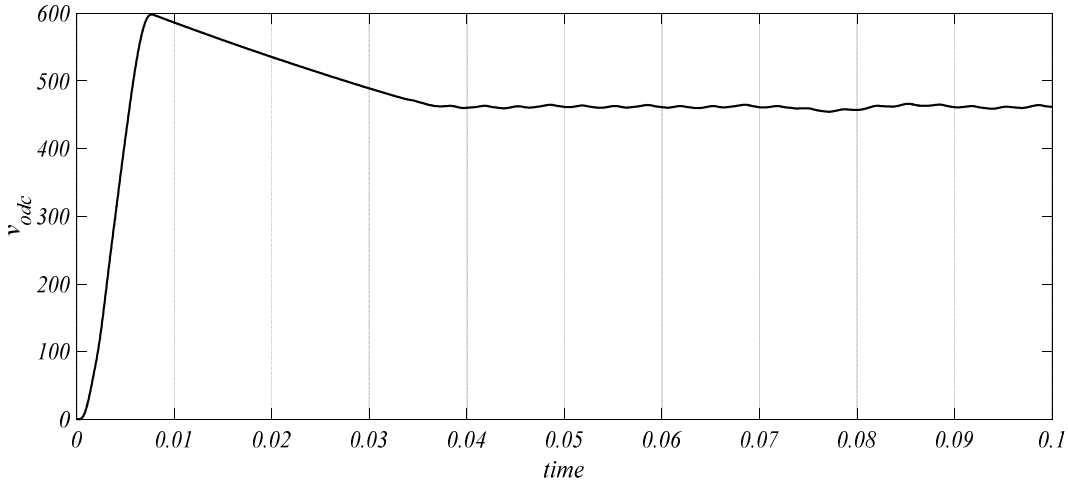

Fig. 6. The DC output voltage (V_{odc}) from the bridge rectifier with non-linear load

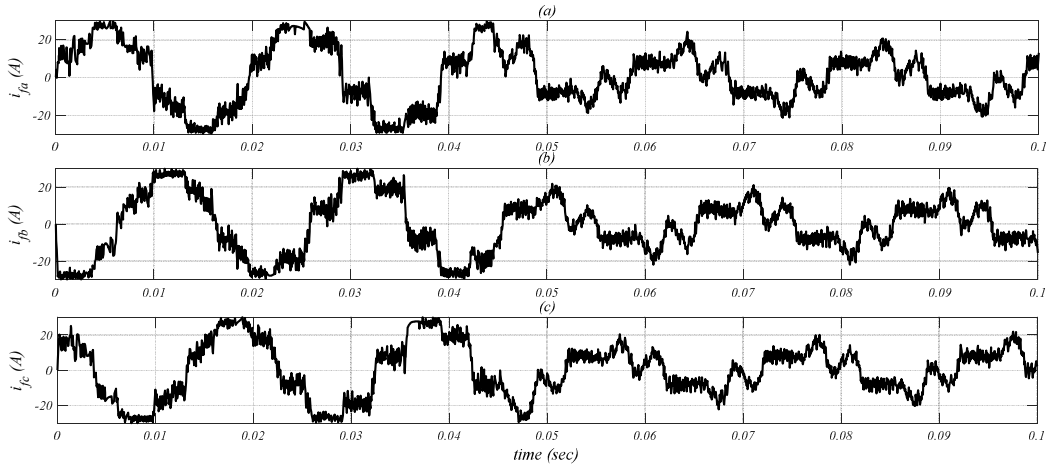

Fig. 7. The inductor filter current ($\boldsymbol{i_f}$) of the three phases with constraint (a) Phase a, (b) phase b, (c) phase c

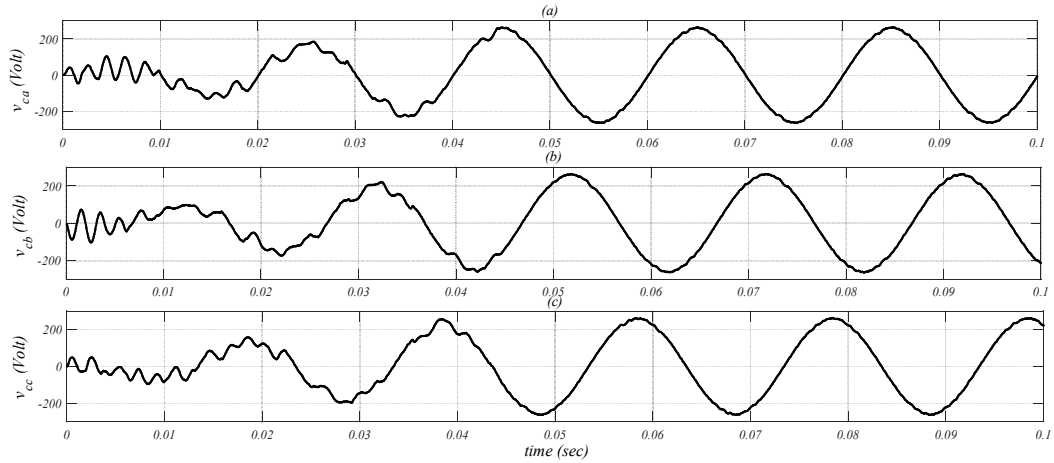

Fig. 8. The output voltage ($\boldsymbol{v}_c$) of the three phases with constraint (a) Phase a, (b) phase b, (c) phase c

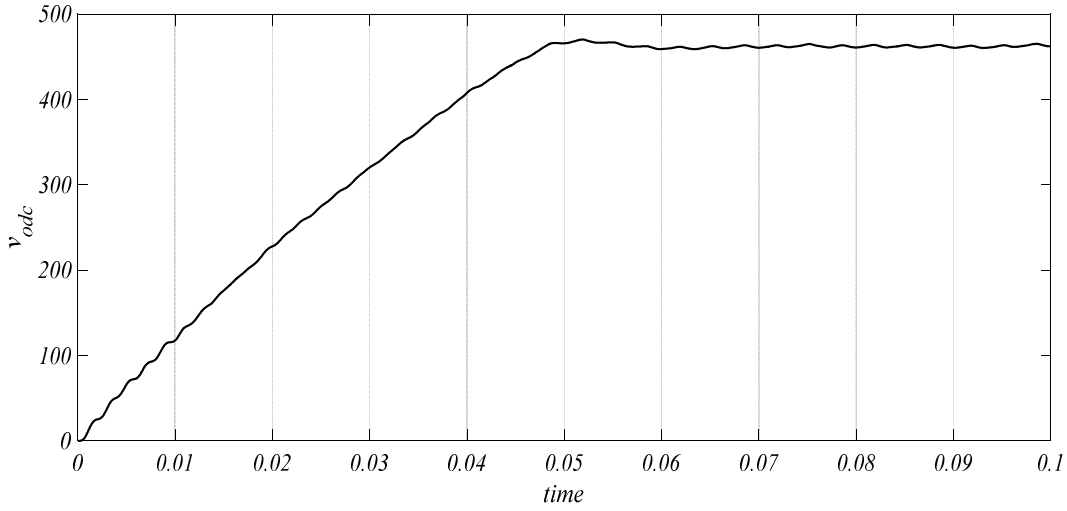

Fig. 9. The DC output voltage (V_{odc}) from the bridge rectifier with constraint load

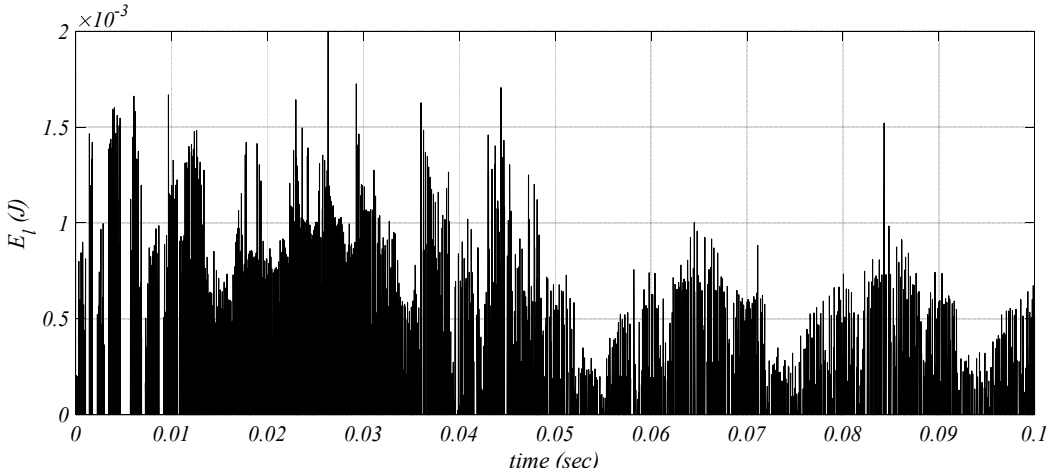

Fig. 10. Energy losses during the switching process with constraint

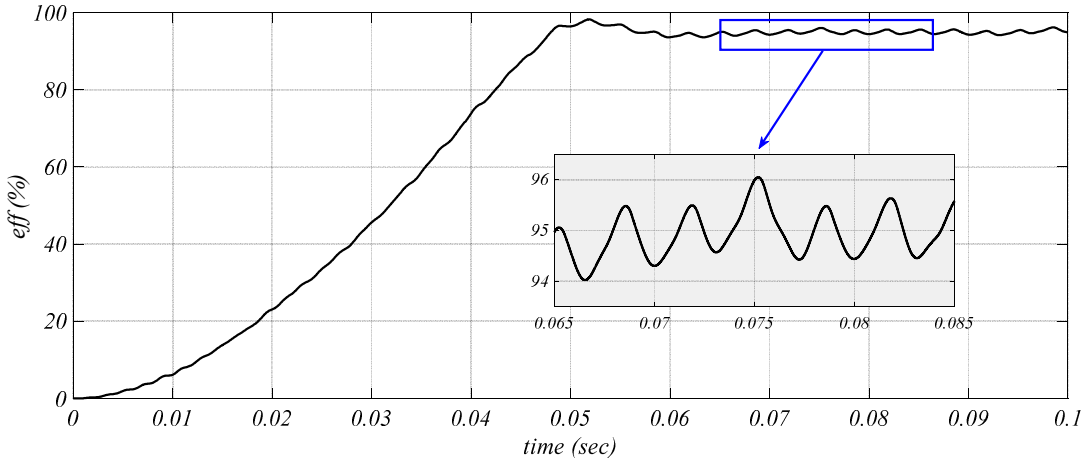

Fig. 11. Efficiency of the system with constraint

V. CONCLUSIONS

Model Predictive Control (MPC) is easy to implement and can efficiently deal with nonlinearity and constraints. It has been shown in the paper that the proposed system achieves good load voltage regulation with low THD and fast transient response with non-linear loads. Here, a constraint is added to limit the inductor filter currents with non-linear load to its maximum steady-state value.

It is worth noting that the FCS-MPC does not require PWM modulator to produce the switching signals of the inverter. But the output of the controller itself is the switching signals according to which the voltage vector of each switching state is selected to minimize the cost function.

REFERENCES

[1] M. Kojima, K. Hirabayashi, Y. Kawabata, E.C. Ejiogu, and T. Kawabata "Novel vector control system using deadbeat-controlled PWM inverter with output LC filter," IEEE Transactions on Industry Applications, Vol. 40, No. 1, pp. 162–169, February 2004.

[2] P. C. Loh, M. J. Newman, D.N. Zmood, and D.G. Holmes, "A comparative analysis of multiloop voltage regulation strategies for single and three phase UPS systems," IEEE Transactions on Power Electronics, Vol. 18, No. 5, pp. 1176–1185, September 2003.

[3] A. Kulka, T. Undeland, S. Vazquez, and L. G. Franquelo, "Stationary frame voltage harmonic controller for standalone power generation," European Conf. Electronics and Applications (EPE'07), Aalborg, Denmark, pp. 1–10, September 2007.

[4] M. N. Marwali, and A. Keyhani, "Control of distributed generation systems-part i: Voltages and currents control," IEEE Transactions on Power Electronics, Vol. 19, No. 6, pp. 1541–1550, November 2004.

[5] G. Escobar, A. A. Valdes, J. Leyva-Ramos, and P. Mattavelli, "Repetitive based controller for a UPS inverter to compensate unbalance and harmonic distortion," IEEE Transactions on Industrial Electronics, Vol. 54, No. 1, pp. 504–510, February 2007.

[6] G. Escobar, P. Mattavelli, A. M. Stankovic, A. A. Valdez, and J. Leyva-Ramos "An adaptive control for UPS to compensate unbalance and harmonic distortion using a combined capacitor/load current sensing," IEEE Transactions on Industrial Electronics, Vol. 54, No. 2, pp. 839–847, April 2007.

[7] Y. Elthokaby, A. E. Elshafei, N. Abdel-Rahim, and E. S. Abdel-Aliem, "Finite-control set model-predictive control for single-phase voltage-source UPS inverters," 18th International Middle East Power Systems Conf. (MEPCON), Cairo, Egypt, pp. 261–265, December 2016.

[8] P. Cortés, M. P. Kazmierkowski, R. M. Kennel, D. E. Quevedo, and J. Rodríguez, "Predictive Control in Power Electronics and Drives," IEEE Transactions on industrial electronics, Vol. 55, No. 12, pp. 4312–4324, December 2008.

[9] J. Holtz, S. Stadtfeld, "A predictive controller for the stator current vector of AC machines fed from a switched voltage source," Proc. IPEC, Tokyo, Japan, pp. 1665–1675, 1983.

[10] M. Depenbrock, "Direct Self-Control (DSC) of inverter-fed induction machine," IEEE Transaction on Power Electronics, Vol. 3, No. 4, pp. 420–429, October 1988.

[11] E. Flach, R. Hoffmann, and P. Mutschler, "Direct mean torque control of an induction motor," Proc. Conf. Rec. EPE, Trondheim, Norway, pp. 672–677, 1997.

[12] P. Mutschler, "A new speed-control method for induction motors," Proc. Conf. Rec. PCIM, Nuremberg, Germany, pp. 131–136, May 1998.

[13] S. Vazquez, J. Leon, L. G. Franquelo, J. Rodriguez, H. A. Young, A. Marquez, and P. Zanchetta, "Model Predictive Control A Review of Its Applications in Power Electronics," IEEE industrial electronics magazine, Vol. 8, No. 1, pp. 16–31, March 2014.

[14] P. Cortés, G. Ortiz, J. I. Yuz, J. Rodríguez, S. Vazquez, and L. G. Franquelo, "Model Predictive Control of an Inverter With Output LC Filter for UPS Applications," IEEE Transactions on industrial electronics, Vol. 56, No. 6, pp. 1875–1883, June 2009

[15] R. P. Aguilera, P. Lezana, and D. E. Quevedo, "Finite-Control-Set Model Predictive Control with Improved Steady-State Performance," IEEE Transactions on industrial informatics, Vol. 9, No. 2, pp. 658–667, May 2013.

[16] J. Rodríguez, J. Pontt, C. A. Silva, P. Correa, P. Lezana, P. Cortés, and U. Ammann, "Predictive Current Control of a Voltage Source Inverter," IEEE Transactions on industrial electronics, Vol. 54, No. 1, pp. 495–503, February 2007.

[17] J. Rodriguez, M. P. Kazmierkowski, J. R. Espinoza, P. Zanchetta, H. Abu-Rub, H. A. Young, and C. A. Rojas, "State of the Art of Finite Control Set Model Predictive Control in Power Electronics," IEEE Transactions on Industrial Informatics, Vol. 9, No. 2, pp. 1003–1016, May 2013.

[18] J. Rodriguez, and P. Cortes, *Predictive control of power converters and electrical drives* John Wiley & Sons, 2012.

[19] P. Cortes, J. Rodriguez, S. Vazquez, and L. G. Franquelo, "Predictive Control of a Three-Phase UPS Inverter Using Two Steps Prediction Horizon," *IEEE International Conference on Industrial Technology*, pp. 1283-1288, March 2010.

[20] S. Kouro, P. Cortes, R. Vargas, U. Ammann, and J. Rodríguez, "Model Predictive Control-A Simple and Powerful Method to Control Power Converters," IEEE Transactions on Industrial Electronics, Vol. 56, No. 6, pp. 41 – 49, June 2009.

[21] F. Schafmeister, C. Rytz, and J. Kolar, "Analytical calculation of the conduction and switching losses of the conventional matrix converter and the (very) sparse matrix converter," Conference Record of Applied Power Electronics Conference and Exposition, APEC 2005, pp. 875–881, March 2005.

[22] R. Vargas, U. Ammann, and J. J. Rodriguez, "Predictive approach to increase efficiency and reduce switching losses on matrix converters," IEEE Transactions on Power Electronics, Vol. 24, No. 4, pp. 894–902, April 2009.

[23] www.onsemi.com